Title
Quantification of liver perfusion using multidelay pseudocontinuous arterial spin labeling

Journal
Journal of Magnetic Resonance Imaging, 43(5)

ISSN
1053-1807

Authors
Pan, Xinlei
Qian, Tianyi
Fernandez-Seara, Maria A
et al.

Publication Date
2016-05-01

DOI
10.1002/jmri.25070

Peer reviewed

Quantification of Liver Perfusion Using Multidelay Pseudocontinuous Arterial Spin Labeling

Xinlei Pan, BS,[1] Tianyi Qian, PhD,[2] Maria A. Fernandez-Seara, PhD,[3] Robert X. Smith, PhD,[4] Kuncheng Li, MD, PhD,[5] Kui Ying, PhD,[6] Kyunghyun Sung, PhD,[7] and Danny J.J. Wang, PhD, MSCE[4,7]*

Purpose: To develop a free-breathing multidelay pseudocontinuous arterial spin labeling (pCASL) technique for quantitative measurement of liver perfusion of the hepatic artery and portal vein, respectively.
Materials and Methods: A navigator-gated pCASL sequence with balanced steady-state free precession (bSSFP) readout was developed and applied on five healthy young volunteers at 3T. Two labeling schemes were performed with the labeling plane applied on the descending aorta above the liver, and perpendicular to the portal vein before its entry to liver to label the hepatic artery and portal vein, respectively. For each labeling scheme, pCASL scans were performed at five or six postlabeling delays between 200 and 2000 msec or 2500 msec with an interval of 400 or 500 msec. Multidelay pCASL images were processed offline with nonrigid motion correction, outlier removal, and fitted for estimation of liver perfusion and transit time.
Results: Estimated liver perfusion of the hepatic artery and hepatic portal vein were 21.8 ± 1.9 and 95.1 ± 8.9 mL/100g/min, with the corresponding transit time of 1227.3 ± 355.5 and 667.2 ± 85.0 msec, respectively. The estimated liver perfusion and transit time without motion correction were less reliable with greater residual variance compared to those processed with motion correction ($P < 0.05$).
Conclusion: The liver perfusion measurement using multidelay pCASL showed good correspondence with values noted in the literature. The capability to noninvasively and selectively label the hepatic artery and portal vein is a unique strength of pCASL as compared to other liver perfusion imaging techniques, such as computed tomography perfusion and dynamic contrast-enhanced MRI.

J. MAGN. RESON. IMAGING 2015;00:000–000.

Liver diseases afflict more than 30 million people in the US, or 1 in 10 Americans.[1] The number of people diagnosed with liver diseases such as hepatitis C, nonalcoholic fatty liver disease, and liver cancer are on the rise both in the US and worldwide.[2] Liver ultrasonography and magnetic resonance imaging (MRI) are the two main imaging modalities for detecting, characterizing, and monitoring treatment responses of focal and diffuse liver diseases.[3–5] Ultrasonography remains the first-line imaging modality for examining liver morphology and blood flow; these are accentuated through the recent development of elastography. MRI offers multiparametric examinations of the morphology, perfusion, and diffusion of the liver. Dynamic contrast-enhanced (DCE) MRI and MR elastography (MRE) are two emerging technologies capable of quantitative assessments of liver perfusion/permeability and viscoelasticity, respectively.

Liver perfusion imaging is useful in detecting regional and global alterations in liver blood flow caused by a range

View this article online at wileyonlinelibrary.com. DOI: 10.1002/jmri.25070

Received Jul 4, 2015, Accepted for publication Sep 24, 2015.

*Address reprint requests to: D.J.J.W., Laboratory of Functional MRI Technology (LOFT), Department of Neurology, UCLA, 660 Charles E Young Dr. South, Los Angeles, CA 90095. E-mail: jwang71@gmail.com

From the [1]Department of Biomedical Engineering, Tsinghua University, Beijing, China; [2]Siemens Healthcare, MR Collaboration NE Asia, Beijing, China; [3]Neuroimaging Laboratory, Division of Neuroscience, Center for Applied Medical Research, University of Navarra, Spain; [4]Laboratory of Functional MRI Technology (LOFT), Department of Neurology, University of California Los Angeles, Los Angeles, California, USA; [5]Department of Radiology, Xuanwu Hospital of Capital Medical University, Beijing, China; [6]Department of Engineering Physics, Tsinghua University, Beijing, China; and [7]Department of Radiology, University of California Los Angeles, Los Angeles, California, USA.

Additional Supporting Information may be found in the online version of this article.

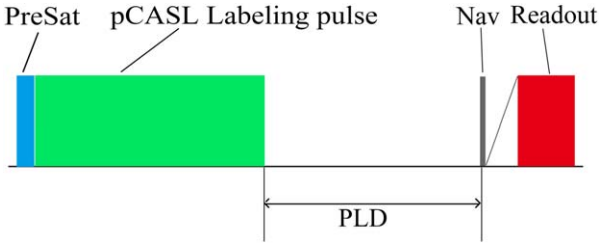

FIGURE 1: Pulse sequence diagram of the proposed free-breathing pCASL sequence for liver perfusion imaging. The sequence is composed of a presaturation pulse followed by the pCASL labeling pulse. After the PLD, a navigator pulse is applied followed by the bSSFP readout with a train of 20 ramp RF pulses.

of focal and diffuse liver diseases. One important goal of liver perfusion imaging is to measure hepatic arterial and portal venous blood flow separately in order to improve the sensitivity and specificity for the diagnosis of liver diseases.[4] In the normal liver, about three-quarters of the blood supply is provided by the portal vein and about one-quarter is provided by the hepatic artery.[5,6] Certain liver diseases such as cirrhosis and liver carcinoma can cause both regional and global liver perfusion changes.[7] It has been shown that malignant neoplasms growing in the liver are largely or exclusively arterial, thus indicating the possibility of arterial blood perfusion imaging to detect liver tumors.[8,9] In liver fibrosis and cirrhosis, a decrease of portal and total hepatic perfusion is observed, as well as increases of arterial perfusion and mean transit time, with preserved or increased distribution volume.[10,11]

To date, however, quantitative liver perfusion imaging remains challenging in clinical settings. For liver perfusion assessment using DCE-MRI, the dynamic curves should be analyzed with a dual-input model, because the liver has two vascular inputs through the hepatic artery and the portal vein.[12] Such kinetic modeling requires both high spatial and temporal resolutions of DCE-MRI with resilience to respiratory motion and other physiological fluctuations. Due to these limitations, most existing studies have employed qualitative assessments during the arterial and hepatobiliary phase of contrast enhancement. In addition, contrast agents may induce adverse reactions in patients with renal dysfunction. Liver ultrasonography can only provide information on global liver blood flow and may be operator-dependent.

Arterial spin labeling (ASL) is a noninvasive MRI technique that can provide quantitative measurements of microvascular blood flow or perfusion by using magnetically labeled blood water as an endogenous tracer. Recent developments in ASL technologies such as pseudocontinuous ASL (pCASL)[13] have provided relatively reliable assessments of cerebral blood flow (CBF) or brain perfusion in a variety of neurologic and psychiatric diseases.[14] However, the application of pCASL on other organs, and in particular for liver perfusion imaging, has been limited.

The purpose of the present study was to investigate a free-breathing liver perfusion imaging protocol by selectively labeling the hepatic artery and portal vein using multidelay pCASL scans in conjunction with a navigator-gated balanced steady-state free precession (bSSFP) readout and nonrigid image registration performed offline.[15]

Materials and Methods

Pulse Sequence

This study was approved by Institutional Review Board, and written informed consents were obtained from all participants before the MR experiment. Five healthy volunteers (age 21–24, 3 males) participated in the MR experiments on a 3T MR (Magnetom TIM Trio, Siemens, Erlangen, Germany) using the body coil as transmitter and the body array flex coil as receiver.

Figure 1 shows the diagram of the pulse sequence. pCASL with balanced gradients between label and control acquisitions was used in combination with a navigator-gated bSSFP readout sequence.[16] The pulse sequence consisted of a presaturation pulse applied on the imaging slice, followed immediately by the pCASL pulse train, and a postlabeling delay (PLD) between the labeling pulse and the bSSFP readout with centric order of *k*-space acquisitions. The bSSFP readout was preceded by a train of 20 dummy radiofrequency (RF) pulses with ramp flip angles to minimize transient signal oscillations. The navigator-echo was applied right

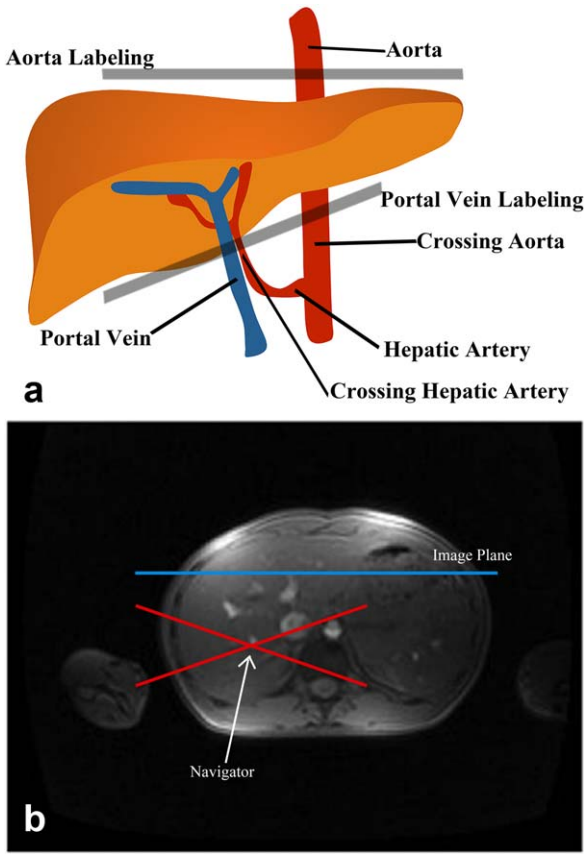

FIGURE 2: Labeling schemes of hepatic artery and hepatic portal vein (a). "Pencil-beam" navigator applied on the right diaphragm (b).

before the bSSFP readout to monitor respiratory motion, which is formed by a spin-echo "pencil-beam" placed on the right diaphragm without intersecting the imaging plane (see Fig. 2).

MRI Experiment

Two series of multidelay pCASL scans were performed on each subject to measure the blood flow from the hepatic artery and portal vein. As shown in Fig. 2a, the labeling plane (blue line) was graphically placed at an approximately perpendicular angle on the descending aorta (above the liver) and the portal vein (before its entry into liver) correspondingly. Note that the former scheme (hereafter termed Scheme A) labels the blood in the hepatic artery only, while the latter scheme (hereafter termed Scheme B) labels the blood in the portal vein (Fig. 2a). In Scheme B, although the labeling plane intersects both the descending aorta and hepatic artery, it causes minimal labeling of the blood in the hepatic artery (see Simulation below). Therefore, Scheme B primarily labels the blood in the portal vein. A single coronal slice was acquired with the following imaging parameters: TR = 4000 msec, field of view (FOV) = 350 mm, matrix size = 128 * 128, slice thickness = 8 mm, rate-2 GRAPPA, centric ordering, labeling duration = 1500 msec, TR/TE of bSSFP = 3.8/1.9 msec, 30 acquisitions (15 pairs label/control images) for each PLD. In each of the five subjects, pCASL scans were implemented with five or six PLDs between 200 and 2000 msec or 2500 msec with an interval of 400 or 500 msec. The scan time for a single PLD was about 5 minutes with ~50% acceptance rate of navigator echoes (±5 mm range of the diaphragm position at the end of expiration).

Bloch Equation Simulations

In the labeling Scheme B, arterial blood flowing through the descending aorta into the hepatic artery will experience a double inversion. Bloch equation simulations were performed to estimate the effect of this double inversion on the flowing spins magnetization. Numerical integration of the Bloch equations was performed using the approach proposed by Maccotta et al.[17] The length of the hepatic artery was assumed to be 3 cm from its root at the descending aorta to the entry of liver.[18] The mean blood flow velocity in the hepatic artery was assumed to be 30 cm/s (~60 cm/s at peak systole and <20 cm/s at diastole).[19] pCASL parameters were identical to those used in the pulse sequence (average RF amplitude = 18 mT, average G strength = 0.6 mT/m, ratio of maximum to average G strength = 10). T_1 and T_2 relaxation values of 1650 and 175 msec, respectively,[20] were assumed for arterial blood at 3T. A parabolic velocity distribution, corresponding to laminar flow, was assumed, with velocities ranging from 0 at the vessel wall to a maximum velocity of 60 cm/s at the center of the vessel, with an average velocity of 30 cm/s. The efficiency was first calculated for each individual velocity. Finally, a weighted average of the efficiencies was computed, taking into account the flow distribution. Simulations were carried out for the label and control conditions.

Data Processing and Analysis

Motion correction was performed for both control and label images during offline postprocessing. The advanced normalization tools (ANTs: http://www.picsl.upenn.edu/ANTS) were used to correct for nonrigid body motion in liver ASL MRI by utilizing a cross-correlation-based symmetric diffeomorphic transformation between the average template and the target time series images.[21] Perfusion-weighted images were obtained by pairwise subtraction of motion-corrected control and label images. Spikes (or outliers) in the difference image series were removed once identified as beyond 2 standard deviations from the mean value (of the 15 difference images of each PLD) and were excluded, and an average perfusion-weighted image was generated for each PLD.[15,22] For comparison, perfusion images were generated without motion correction using ANTs but with the outlier removal as described above. Several hand-drawn regions of interest (ROIs) of liver tissue (excluding visible vasculature) were used for measuring the mean difference signals,[23] which were used to fit blood flow and transit time based on the following two-compartment model[24]:

$$dM = -\frac{2M_0 f \alpha}{\lambda}\left\{\begin{array}{l}\dfrac{\exp(-\delta R_{1a})}{R_{1app}}\left[\exp\Big(\min(\delta-w,0)R_{1app}\Big)-\exp\Big((\delta-\tau-w)R_{1app}\Big)\right] \\ +\dfrac{1}{R_{1a}}\left[\exp\Big(\Big(\min(\delta_a-w,0)-\delta_a\Big)R_{1a}\Big)-\exp\Big(\Big(\min(\delta-w,0)-\delta\Big)R_{1a}\Big)\right]\end{array}\right\} \quad (1)$$

where dM is the pCASL difference signal (label-control); M_0 is the equilibrium liver tissue magnetization (control image intensity); f is liver perfusion; λ is the blood/tissue water partition coefficient (0.9 for both brain and abdominal tissues)[25]; α is the tagging efficiency of pCASL, and the value is 0.85[16]; δ is the transit time from the labeling region to the tissue compartment, and δ_a is the transit time from the labeling region to the vascular compartment; τ is the tagging duration; w is the time interval between the labeling pulse and image acquisition; R_{1a} is the longitudinal relaxation rate of blood (1/1664 msec^{-1} and 1/1585 msec^{-1} for hepatic artery and portal vein, respectively),[26] and $R_{1app} = R_1 + f/\lambda$, where R_1 is the longitudinal relaxation rate of liver tissue in the absence of blood flow, the value is 1/809 msec^{-1},[27] and the min ( ) function returns the smallest of its input arguments.

Since the fitting of three parameters f, δ, and δ_a was not reliable, we made the assumption that the labeled blood spends minimal time in the vascular compartment and immediately exchanges into liver tissue once it reaches the imaging pixel (ie, $\delta_a = \delta$). This is a reasonable assumption since, unlike the water exchange in the brain that has to go through the blood–brain barrier, there are no

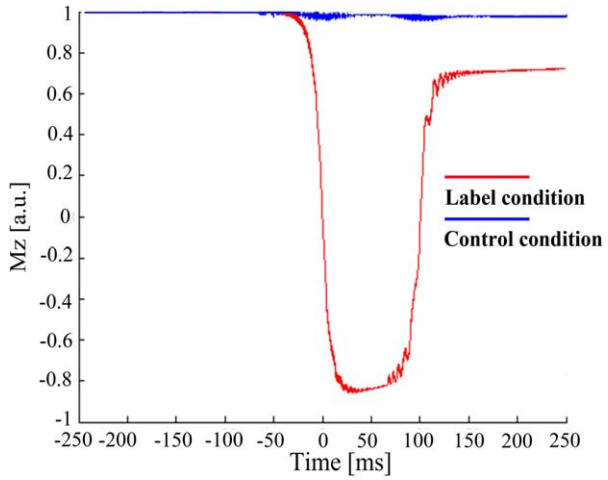

FIGURE 3: Evolution of the longitudinal component of the magnetization of arterial blood (Mz) as it flows through the labeling plane in Scheme B at a mean velocity of 30 cm/s, experiencing a double inversion during the label condition (in red). During the control condition (in blue), the effect is negligible. The x-axis represents time, with time = 0, corresponding to the first crossing through the labeling plane.

tight junctions between endothelial cells in the blood vessels of the systemic circulation. Therefore, Eq. (1) can be simplified to Eq. (2) with two unknown parameters f and δ or transit time.

$$dM = -\frac{2M_0 f \alpha}{\lambda}\left\{\frac{\exp(-\delta R_{1a})}{R_{1app}} \times \left[\exp\left(\min(\delta - w, 0)R_{1app}\right) - \exp\left((\delta - \tau - w)R_{1app}\right)\right]\right\} \quad (2)$$

Data fitting was implemented in MatLab (MathWorks, Natick, MA) using the curve-fitting toolbox. The nonlinear least squares method was used to fit the perfusion model to the dynamic perfusion data. The fitting algorithm was Trust-region; The lower and upper bounds for the hepatic aorta blood perfusion value were 10 mL/(100g*min) and 60 mL/(100g*min), respectively, and for the hepatic portal vein were 80 mL/(100g*min) and 200 mL/(100g*min), respectively; The lower and upper bounds for the arterial transit time were (0.1, 5 sec) for labeled aorta and (0.1, 3 sec) for labeled portal vein, respectively. The maximum and minimum change in coefficients for finite difference gradients were 1e-1 and 1e-8, respectively. The maximum number of iterations allowed and the maximum number of function (model) evaluations allowed were both 10,000,000. The termination tolerance on the function (model) value was set at 1e-6.

Results

Bloch Equation Simulation

The estimated labeling efficiency of the "double inversion" of arterial blood in descending aorta and hepatic artery in Scheme B was 8.3% during the label condition and 0.8% during the control condition. Figure 3 clearly shows this double inversion of the arterial blood as it flows from descending aorta to the hepatic artery, for a mean velocity of 30 cm/s. The first inversion takes place at time zero (when the arterial blood crosses the inversion plane for the first time). After this inversion Mz experiences longitudinal (T_1) relaxation and the absolute magnitude of Mz decreases with T_1. The arterial blood in the hepatic artery crosses the labeling plane a second time. In the simulations, the length

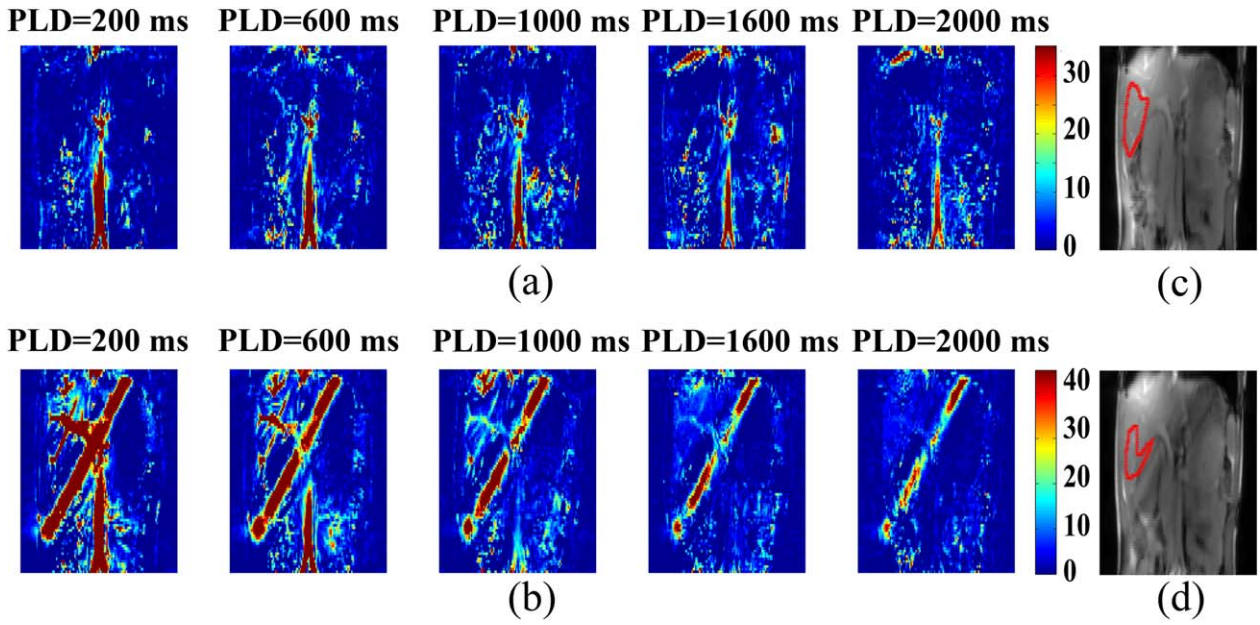

FIGURE 4: Perfusion weighted images at multiple PLDs. Aorta labeled (a) (the color scale indicates the magnitude of difference perfusion signal (AU), the same for (b)); portal vein labeled (b); Anatomic image for aorta labeled with ROI delineated (c); anatomic image for portal vein labeled with ROI delineated (d). Note the diagonal bright lines in (b) are caused by the labeling plane.

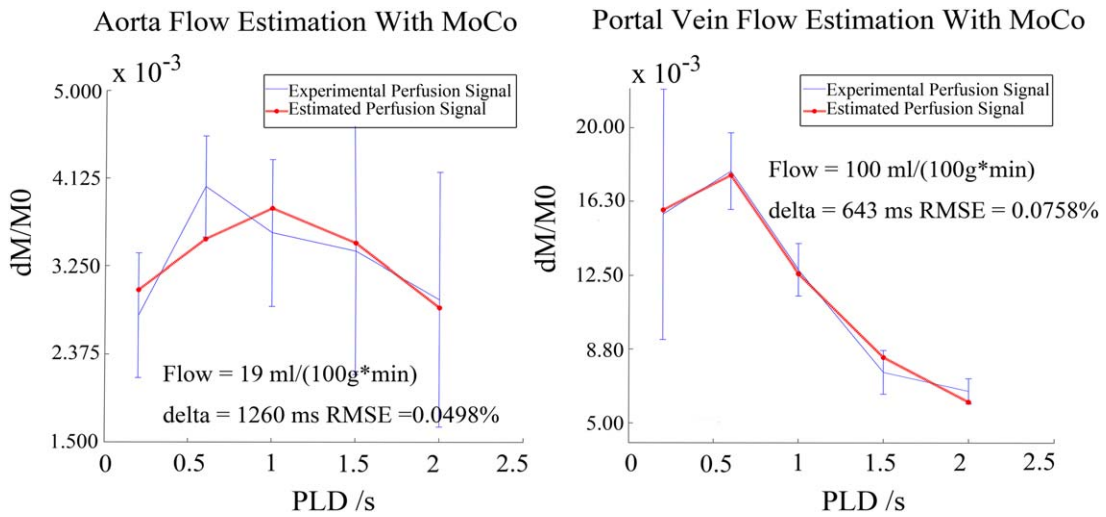

FIGURE 5: Model fitting results with motion correction: Mean fractional difference perfusion signal (dM/M0) measured in hepatic aorta (left) and hepatic portal vein (right). In vivo (blue line) and estimated data (red line) are shown and error bars indicate standard deviation.

of the hepatic artery from its root at the descending aorta to the entry of the liver was considered to be 3 cm. Therefore, with a velocity of 30 cm/s it takes 100 msec for the blood to travel from the location of the first crossing to the second crossing. At time 100 msec, the second inversion inverts the Mz component that goes from a negative value to a positive value. Following this second inversion, Mz experiences longitudinal relaxation to its equilibrium value. Note that the labeling efficiency of the "single inversion" using pCASL was 85%.

In Vivo Experiment Results

A representative example of the series of perfusion-weighted images across multiple PLDs is shown in Fig. 4. Liver perfusion can be seen in long PLD (≥1.6 sec) images especially for portal vein labeling. Typical average difference perfusion signal (dM) curves processed with motion correction of the two labeling schemes are shown in Fig. 5. The dM signals are expressed as the ratio of the difference perfusion signal (dM) over the equilibrium liver tissue signal (M_0). As can be seen, the average fractional hepatic artery and portal vein signals show an initial upward trend followed by a downward trend because of the transit delay. For comparison, the average difference perfusion signal curves processed without motion correction of the two labeling schemes are shown in Fig. 6. The model fitting results of a representative subject are shown in Fig. 7, processed with (Fig. 7a) and without (Fig. 7b) offline motion correction, respectively. The difference perfusion images of a representative subject processed

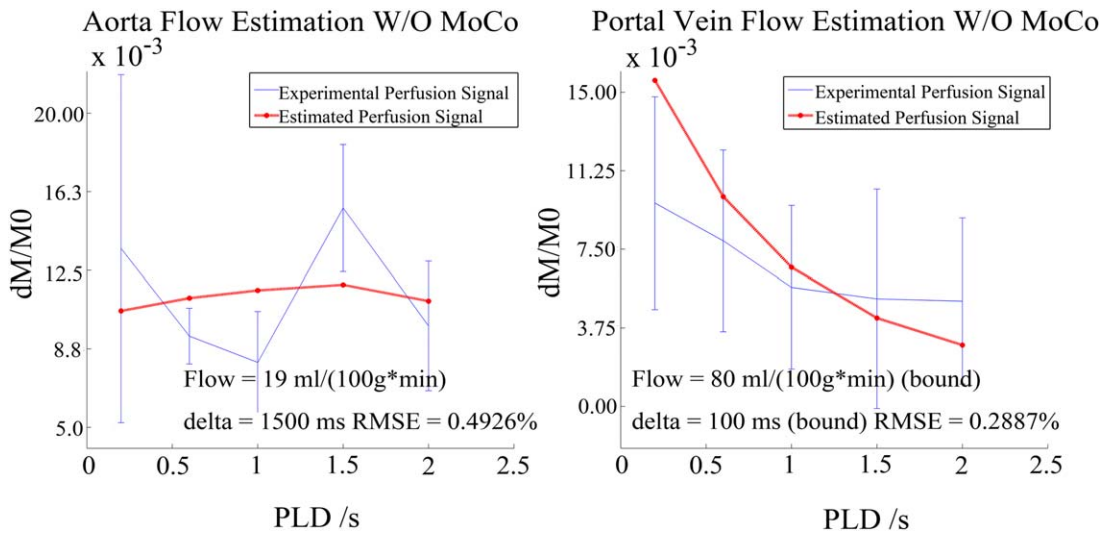

FIGURE 6: Model fitting results without motion correction: Mean fractional difference perfusion signal (dM/M0) measured in hepatic aorta (left) and hepatic portal vein (right). In vivo (blue line) and estimated data (red line) are shown and error bars indicate standard deviation.

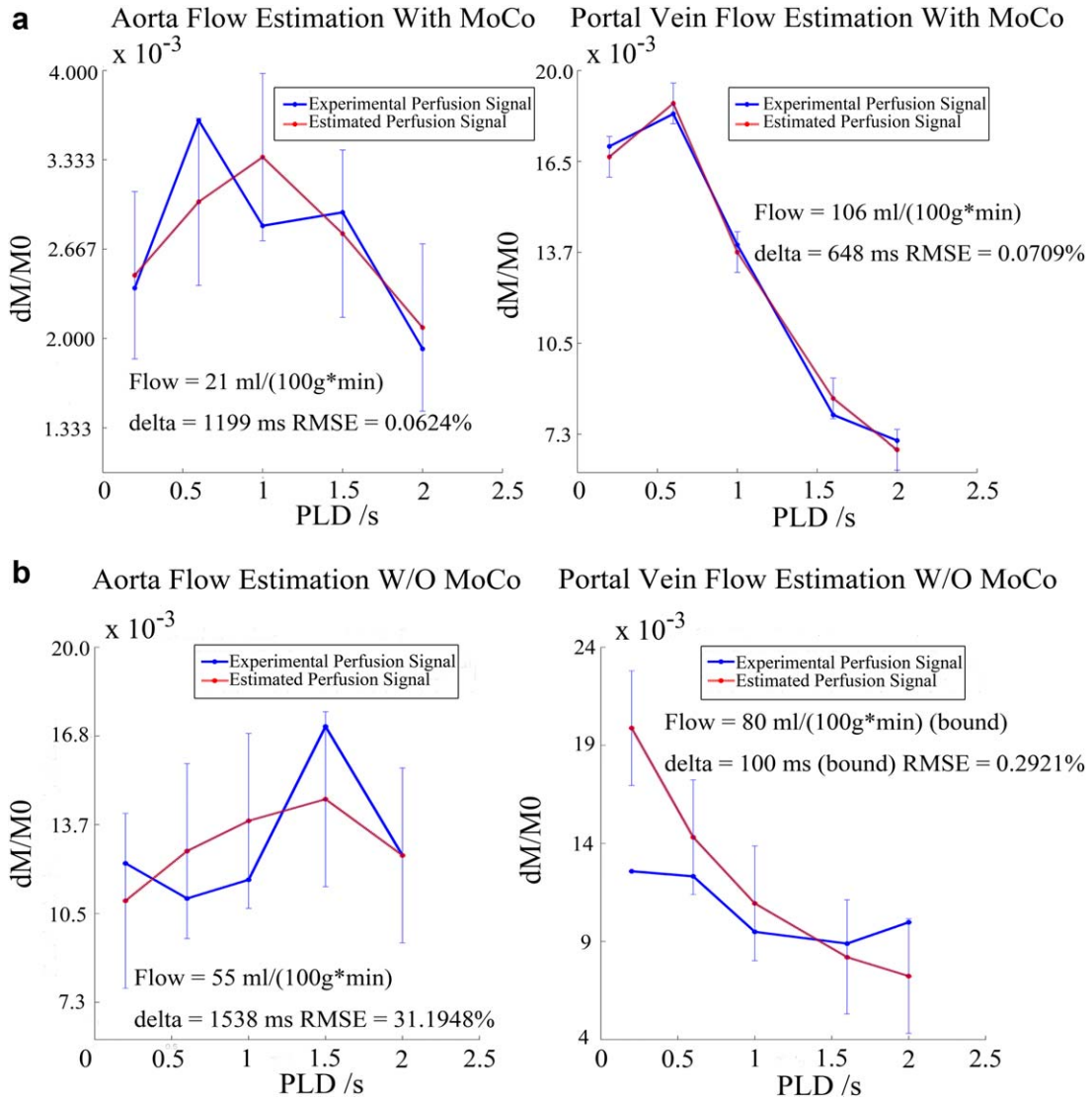

FIGURE 7: Model fitting results of a representative subject: with motion correction (a); without motion correction (b).

TABLE 1. Estimated Liver Perfusion Value and Transit Time (With Motion Correction)

Subject number (age, gender)	Blood flow (ml/(100g*min))		Transit time		Root mean square error (%)	
	Hepatic artery labeled	Portal vein labeled	Hepatic artery labeled	Portal vein labeled	Hepatic artery labeled	Portal vein labeled
Subject 1 (21, M)	21.0	105.7	1196.2	647.7	0.0625	0.0708
Subject 2 (23, M)	18.9	99.2	1124.8	808.3	0.1447	0.0842
Subject 3 (24, M)	24.0	97.0	1810.7	671.4	0.0175	0.2668
Subject 4 (21, F)	22.5	91.6	840.4	622.9	0.0455	0.2062
Subject 5 (23, F)	22.6	82.0	1164.2	585.8	0.0312	0.1091
Mean ± SD	21.8 ± 1.9	95.1 ± 8.9	1227.3 ± 355.5	667.2 ± 85.0	0.0603 ± 0.0501	0.1474 ± 0.0852

TABLE 2. Estimated Liver Perfusion Value and Transit Time (W/O Motion Correction)

Subject number (age, gender)	Blood flow (ml/(100g*min))		Transit time		Root mean square error (%)	
	Hepatic artery labeled	Portal vein labeled	Hepatic artery labeled	Portal vein labeled	Hepatic artery labeled	Portal vein labeled
Subject 1 (21, M)	23.8	80.0 (bound)	2231.7	853.9	0.3511	0.3154
Subject 2 (23, M)	51.6	80.0 (bound)	809.3	1107.6	0.5111	0.3759
Subject 3 (24, M)	10.0 (bound)	80.0 (bound)	100.0(bound)	702.4	0.8126	0.4080
Subject 4 (21, F)	33.8	80.0 (bound)	2783.9	876.8	0.4401	0.1935
Subject 5 (23, F)	11.3	80.0 (bound)	200.0	2375.8	0.3117	1.1839
Mean ± SD	26.1 ± 17.3	80.0 ± 0.0	1225.0 ± 1217.9	1183.3 ± 682.2	0.4853 ± 1.1987	0.4953 ± 0.3935

with and without motion correction are displayed in Supporting Fig. 1. The residual motion artifacts along the upper edge of the liver in perfusion images processed without motion correction are removed in perfusion images processed with motion correction.

The results of quantitative model fitting for each subject are listed in Tables 1 and 2, processed with motion correction (MoCo) and without motion correction (W/O MoCo), respectively. Estimated mean blood flow of hepatic artery labeled data is (mean ± SD) 21.8 ± 1.9 mL/(100g*min) and is 95.1 ± 8.9 mL/(100g*min) for hepatic portal vein labeled data. The estimated transit time is 1227.3 ± 355.5 and 667.2 ± 85.0 msec for the hepatic artery and portal vein, respectively. For images processed without motion correction, the estimated perfusion is 26.1 ± 17.3 and 80.0 ± 0.0 mL/(100g*min), and transit time is 1225.0 ± 1217.9 and 1183.3 ± 682.2 msec for the hepatic artery and portal vein, respectively. As can be seen, the model fitting results without motion correction showed much larger variability and residual error (see root mean square error [RMSE] listed in Tables 1, 2) compared to those with motion correction ($P < 0.05$, Wilcoxon signed-rank test). As a matter of fact, the model fitting ended with boundary conditions for all five subjects for portal vein labeled data processed without motion correction.

Discussion

Liver blood supply consists of both hepatic artery and hepatic portal vein, where hepatic artery accounts for about 25% of the blood supply and hepatic portal vein accounts for about 75% of the blood supply.[5] This study demonstrated the feasibility for quantifying liver perfusion of the hepatic artery and hepatic portal vein using a multidelay pCASL sequence. Compared to existing liver perfusion measurement techniques, such as hepatic venous portal pressure gradient measurements (HVPG) and DCE-MRI, the proposed multidelay pCASL technique is entirely noninvasive and can selectively label the hepatic artery and hepatic portal vein, respectively.

Computed tomography (CT) has been used for liver perfusion measurement. Weidekamm et al[28] reported that the mean normal perfusion values measured by single-section CT for hepatic arterial, portal venous, and total perfusion were 20, 102, and 122 mL/min per 100 mL, respectively. However, the high radiation dose of dynamic CT scans such as CT perfusion has become a major concern for patient safety and long-term health. Currently, reliable and accurate liver perfusion imaging using DCE-MRI remains challenging in clinical settings given the requirement of both high spatial and temporal resolutions to differentiate the dual blood circulation in the presence of respiratory motion. In addition, gadolinium (Gd)-based contrast agents are not suitable for patients with renal dysfunction. One

recent DCE-MRI study[29] reported hepatic arterial and portal venous perfusion in the normal liver tissue of patients with intrahepatic cancer to be 22.4 ± 8.0 and 120.5 ± 30.0 mL/100g/min, respectively. The result of perfusion measurement using multidelay pCASL shows good concordance with the literature values by CT perfusion and DCE-MRI.

In addition, nonrigid motion correction of free-breathing abdominal MRI images in conjunction with navigator-gating using "pencil-beam" are helpful to improve the reliability of liver perfusion imaging using pCASL, as shown for myocardium ASL perfusion imaging.[15] In the present study, the estimated liver perfusion using aortic and portal vein labeling was 21.8 ± 1.9 and was 95.1 ± 8.9 mL/100g/min with motion correction. For data processed without nonrigid motion correction, the fitting routine failed to converge in all five subjects for portal vein labeled data and boundary values had to be assumed. The residual errors of model fitting indicated by RMSE values were also much larger for pCASL data processed without motion correction compared to those with motion correction. This indicates the importance of controlling motion both during image acquisition and postprocessing for ASL perfusion imaging of liver and other body organs. The fitted arterial transit times (1227.3 ± 355.5 and 667.2 ± 85.0 msec for the hepatic artery and portal vein, respectively) are also in concordance with literature values on body organs.[25] Since the aortic labeling (Scheme A) is farther away from the liver entry of the hepatic artery ($\sim$15 cm of descending aorta and $\sim$3–4 cm of hepatic artery), the added $\sim$600 msec transit time for the hepatic artery compared to the portal vein is reasonable.

As an initial attempt for noninvasive and quantitative liver perfusion imaging, the present study has a few limitations. First, only a single coronal slice through the liver was imaged using bSSFP to keep the respiratory motion primarily in-plane. Banding artifact was present in a few subjects at the interface between the liver and the diaphragm, although we carefully avoided these regions for ROI analyses. In the future, 3D volumetric imaging sequences with resistance to susceptibility effects such as GRASE (a hybrid of gradient and spin echo) should be applied for liver perfusion imaging.[30] Another caveat of the labeling scheme for hepatic portal vein is that the oblique labeling plane may (partially) label the blood in the hepatic artery due to incomplete "double inversion," although the numerical simulations showed this effect to be small ($\sim$8%). The variations of the geometry and blood flow velocities of the hepatic artery between subjects may also affect the labeling efficiency of the hepatic artery in Scheme B. One potential solution would be to place the labeling plane further away from the liver to avoid the hepatic artery while still labeling the portal vein, with the assistance of MR angiography (MRA).

In conclusion, we presented a free-breathing multidelay pCASL protocol for quantitative liver perfusion imaging of the hepatic artery and portal vein, respectively. The capability to noninvasively and selectively label the hepatic artery and portal vein is a unique strength of pCASL as compared to other liver perfusion imaging techniques such as CT perfusion and DCE-MRI. In the future, the clinical utility of liver perfusion imaging using multidelay pCASL should be evaluated in clinical applications in liver diseases.

Acknowledgements

Contract grant sponsor: National Institutes of Health (NIH); contract grant numbers: U01-HD087221, R01-NS081077, R01-EB014922.

References

1. Schiller JS, Lucas JW, Peregoy JA. Summary health statistics for U.S. adults: national health interview survey, 2011. Vital and Health Statistics, Series 10: Data from the National Health Interview Survey. Centers for Disease Control and Prevention website. www.cdc.gov/nchs/data/series/sr_10/sr10_256.pdf.
2. Williams R. Global challenges in liver disease. Hepatology 2006;44:521–526.
3. Fausto N. Liver regeneration. J Hepatol 2000;32(1 Suppl):19–31.
4. Pandharipande PV, Krinsky GA, Rusinek H, Lee VS. Perfusion imaging of the liver: current challenges and future goals. Radiology 2005;234:661–673.
5. Chiandussi L, Greco F, Sardi G, Vaccarin A, Ferraris CM, Curti B. Estimation of hepatic arterial and portal venous blood flow by direct catheterization of vena porta through umbilical cord in man. Preliminary results. Acta Hepatosplenol 1968;15:166–171.
6. Schenk WG Jr, McDonald JC, McDonald K, Drapanas T. Direct measurement of hepatic blood flow in surgical patients: with related observations on hepatic flow dynamics in experimental animals. Ann Surg 1962;156:463–471.
7. Kim SH, Kamaya A, Willmann JK. CT perfusion of the liver: principles and applications in oncology. Radiology 2014;272:322–344.
8. Liu Y, Matsui O. Changes of intratumoral microvessels and blood perfusion during establishment of hepatic metastases in mice. Radiology 2007;243:386–395.
9. International Consensus Group for Hepatocellular Neoplasia. Pathologic diagnosis of early hepatocellular carcinoma: a report of the international consensus group for hepatocellular neoplasia. Hepatology 2009;49:658–664.
10. Hagiwara M, Rusinek H, Lee VS, et al. Advanced liver fibrosis: diagnosis with 3D whole-liver perfusion MR imaging—initial experience. Radiology 2008;246:926–934.
11. Annet L, Materne R, Danse E, Jamart J, Horsmans Y, Van Beers BE. Hepatic flow parameters measured with MR imaging and Doppler US: correlations with degree of cirrhosis and portal hypertension. Radiology 2003;229:409–414.
12. Bultman EM, Brodsky EK, Horng DE, et al. Quantitative hepatic perfusion modeling using DCE-MRI with sequential breathholds. J Magn Reson Imaging 2014;39:853–865.

13. Dai W, Garcia D, de Bazelaire C, Alsop DC. Continuous flow-driven inversion for arterial spin labeling using pulsed radio frequency and gradient fields. Magn Reson Med 2008;60:1488–1497.

14. Detre JA, Rao H, Wang DJ, Chen YF, Wang Z. Applications of arterial spin labeled MRI in the brain. J Magn Reson Imaging 2012;35:1026–1037.

15. Wang DJJ, Bi XM, Avants BB, Meng TB, Zuehlsdorff S, Detre JA. Estimation of perfusion and arterial transit time in myocardium using free-breathing myocardial arterial spin labeling with navigator-echo. Magn Reson Med 2010;64:1289–1295.

16. Wu WC, Fernandez-Seara M, Detre JA, Wehrli FW, Wang J. A theoretical and experimental investigation of the tagging efficiency of pseudocontinuous arterial spin labeling. Magn Reson Med 2007;58:1020–1027.

17. Maccotta L, Detre JA, Alsop DC. The efficiency of adiabatic inversion for perfusion imaging by arterial spin labeling. NMR Biomed 1997;10:216–221.

18. Sebben GA, Rocha SL, Sebben MA, Parussolo Filho PR, Goncalves BH. Variations of hepatic artery: anatomical study on cadavers. Rev Col Bras Cir 2013;40:221–226.

19. Hubner GH, Steudel N, Kleber G, Behrmann C, Lotterer E, Fleig WE. Hepatic arterial blood flow velocities: assessment by transcutaneous and intravascular Doppler sonography. J Hepatol 2000;32:893–899.

20. Lu H, Xu F, Grgac K, Liu P, Qin Q, van Zijl P. Calibration and validation of TRUST MRI for the estimation of cerebral blood oxygenation. Magn Reson Med 2012;67:42–49.

21. Avants BB, Epstein CL, Grossman M, Gee JC. Symmetric diffeomorphic image registration with cross-correlation: evaluating automated labeling of elderly and neurodegenerative brain. Med Image Anal 2008;12:26–41.

22. Seo S, University of Pittsburgh. Graduate School of Public Health. A review and comparison of methods for detecting outliers in univariate data sets. Pittsburgh: University of Pittsburgh; 2006.

23. Friedman JH, Tukey JW. Projection pursuit algorithm for exploratory data-analysis. IEEE Trans Comput 1974;C 23:881–890.

24. Wang JJ, Alsop DC, Li L, et al. Comparison of quantitative perfusion imaging using arterial spin labeling at 1.5 and 4.0 Tesla. Magn Reson Med 2002;48:242–254.

25. Robson PM, Madhuranthakam AJ, Dai W, Pedrosa I, Rofsky NM, Alsop DC. Strategies for reducing respiratory motion artifacts in renal perfusion imaging with arterial spin labeling. Magn Reson Med 2009;61:1374–1387.

26. Lu H, Clingman C, Golay X, van Zijl PC. Determining the longitudinal relaxation time (T1) of blood at 3.0 Tesla. Magn Reson Med 2004;52:679–682.

27. de Bazelaire CMJ, Duhamel GD, Rofsky NM, Alsop DC. MR imaging relaxation times of abdominal and pelvic tissues measured in vivo at 3.0 T: preliminary results. Radiology 2004;230:652–659.

28. Weidekamm C, Cejna M, Kramer L, Peck-Radosavljevic M, Bader TR. Effects of TIPS on liver perfusion measured by dynamic CT. Am J Roentgenol 2005;184:505–510.

29. Wang H, Cao Y. Correction of arterial input function in dynamic contrast-enhanced MRI of the liver. J Magn Reson Imaging 2012;36:411–421.

30. Wang DJ, Alger JR, Qiao JX, et al. Multi-delay multi-parametric arterial spin-labeled perfusion MRI in acute ischemic stroke — comparison with dynamic susceptibility contrast enhanced perfusion imaging. NeuroImage Clin 2013;3:1–7.